




# Non-structural protein 1 from avian influenza virus H9N2 is an efficient RNA silencing suppressor with characteristics that differ from those of *Tomato bushy stunt virus* p19

Ru Yu<sup>1</sup> · Xiuli Jing<sup>2</sup> · Wenjing Li<sup>1</sup> · Jie Xu<sup>1</sup> · Yang Xu<sup>1</sup> · Liwei Geng<sup>1</sup> · Changxiang Zhu<sup>1</sup> · Hongmei Liu<sup>1</sup> 

Received: 12 May 2017 / Accepted: 19 February 2018 / Published online: 26 February 2018  
© Springer Science+Business Media, LLC, part of Springer Nature 2018

## Abstract

Non-structural protein 1 (NS1) of influenza A virus is a multifunctional dimeric protein that contains a conserved N-terminal RNA binding domain. Studies have shown that NS1 suppresses RNA silencing and the NS1 proteins encoded by different influenza A virus strains exhibit differential RNA silencing suppression activities. In this study, we showed that the NS1 protein from avian influenza virus (AIV) H9N2 suppressed systemic RNA silencing induced by sense RNA or dsRNA. It resulted in more severe *Potato virus X* symptom, but could not reverse established systemic green fluorescent protein silencing in *Nicotiana benthamiana*. In addition, its systemic silencing suppression activity was much weaker than that of p19. The local silencing suppression activity of AIV H9N2 NS1 was most powerful at 7 dpi and was even stronger than that of p19. And the inhibition ability to RNA silencing of NS1 is stronger than that of p19 in human cells. Collectively, these results indicate that AIV H9N2 NS1 is an effective RNA silencing suppressor that likely targets downstream step(s) of dsRNA formation at an early stage in RNA silencing. Although NS1 and p19 both bind siRNA, their suppression mechanisms seem to differ because of differences in their suppression activities at various times post-infiltration and because p19 can reverse established systemic RNA silencing, but NS1 cannot.

**Keywords** Avian influenza virus · RNA silencing suppressor · NS1 · H9N2 · p19

## Introduction

RNA silencing is a highly conserved antiviral mechanism in plant and mammalian cells [1]. As a counter-defence mechanism, viruses may encode specific proteins, known as RNA silencing suppressor (RSS) proteins [2], to target various steps of the silencing pathway [3]. Both animal and plant virus have been shown to encode RSSs. As for its mode of

---

Edited by Thomas Hohn.

---

Ru Yu and Xiuli Jing have contributed equally to this work.

---

✉ Hongmei Liu  
hmliu@sdau.edu.cn

Ru Yu  
angelyuru@163.com

Xiuli Jing  
jingxiuli84@163.com

Wenjing Li  
15165638929@163.com

Jie Xu  
dedeer87@126.com

Yang Xu  
xuyangpgcn@163.com

Liwei Geng  
1187547899@qq.com

Changxiang Zhu  
zhchx@sdau.edu.cn

<sup>1</sup> State Key Laboratory of Crop Biology, College of Life Sciences, Shandong Agricultural University, Tai'an 271018, China

<sup>2</sup> Institute of Immunology, Taishan Medical University, Tai'an 271000, China

action, HC-Pro was reported to reduce the accumulation of siRNAs and sequester double-stranded small RNAs, preventing their incorporation into the RNA-induced silencing complex (RISC) [4]. In addition, HC-Pro may decrease the stability of siRNAs by modifying their 3' overhangs [5]. The 2b protein of *Tomato aspermy virus* was confirmed as an RSS when it was found to bind double-stranded RNAs (dsRNAs) and argonaute proteins [6–8]. The first RSS discovered in an animal virus was B2 protein from flock house virus [9], followed by the  $\sigma$  protein of reovirus, non-structural protein 1 (NS1) from influenza A virus, and E3L protein encoded by vaccinia virus [10].

NS1 has been found to play multiple functions in the process of avian influenza virus (AIV) assembly [11]. NS1 protein, largely synthesized in infected cells at an early stage of AIV infection, contributes to efficient virus accumulation through multiple interactions with proteins or RNAs [12, 13]. As a kind of regulatory protein with versatile functions, NS1 plays a key role in modulating the pathogenicity and replication of influenza virus [14, 15]. Differential gene lengths and protein structures exist in NS1 proteins of different AIV strains. NS1 protein is composed of two functional domains, namely RNA binding domain and effector domain [16]. NS1 can inhibit the transportation of host mRNA from nuclear to cytoplasm, block pre-mRNA splicing by combining the nuclear RNA and restrain dsRNA-dependent protein kinase activation by binding dsRNA, even interact with many host cell proteins [17]. NS1 also functions on the regulation of immune responses. NS1 encoded by human influenza virus was first reported as an RSS [18]. Maliogka et al. showed that NS1 could replace the well-known silencing suppression function of HC-Pro from plant potyvirus [19]. NS1 could also suppress RNA silencing in plants and *Drosophila* [20, 21], and recent studies have shown the activity of NS1 to suppress either the artificially engineered RNAi [22] or the biogenesis of influenza A virus-derived siRNAs in human cells [23]. Site-directed mutagenesis of AIV NS1 indicated that some positively charged residues played key roles in its dsRNA binding [24]. Our previous studies discovered that any mutations of 35R and 46R which contribute to the homodimeric structure of NS1 caused the loss of RSS activity. And the first 70 residues of NS1 could suppress RNA silencing triggered by sense transgene, but this sequence was not sufficient to block dsRNA-induced silencing [25].

In this study, we showed that AIV H9N2 NS1 protein could suppress local and systemic RNA silencing triggered by either sense RNA or dsRNA. Moreover, AIV H9N2 NS1 could not reverse the established systemic GFP silencing, which verified by the PVX vector. Its systemic silencing suppression activity is much weaker than that of p19. However, the RSS activity of AIV H9N2 NS1 was most powerful at about 7 dpi, even stronger than that of p19. Collectively,

AIV H9N2 NS1 is an efficient RSS with a different action mode from p19, although both of them could bind siRNA and probably plays role in the downstream of dsRNA formation at the early stage of RNA silencing.

## Materials and methods

### Plant materials and plasmid constructs

Green fluorescent protein (GFP) transgenic *Nicotiana benthamiana* line 16c plants were grown at  $24 \pm 2$  °C under a 16-h light and 8-h darkness regimen.

*Agrobacterium* clones containing the GFP, p19, and dsGFP expression cassettes have been described previously [26]. The NS1 gene (GQ981533) was amplified by reverse transcription PCR with specific primers NS1-F: CAGGATCCATGGATTCCAACACGTG and NS1-R: CAGAGCTCTCTTCAAACCTTCTGACTCA from total RNA extracted from AIV H9N2 and the resulting PCR product was cloned into the PMD-18T vector (TaKaRa, DaLian, China) to produce PMD-NS1. Then this construct was digested with specific enzymes and cloned between the 35S promoter and the Nos terminator of the binary vector pBI121 to yield construct 35S-NS1. To produce PVX-NS1, the NS1 sequence was amplified from plasmid PMD-NS1 using the primers PVX-NS1-F: GCGCGGCCGCATGGATTCCAACACTGTGTC and PVX-NS1-R: GCGTCGACTCAAACCTTCTGACTCAACCG and then inserted into the *Sall/NotI* site in the PVX vector pGR106. In order to construct pCMV-NS1 and pCMV-p19, the sequences were amplified from plasmid PMD-NS1 and pBI121-p19 using the primers pCMV-NS1-F: GCGAATTCATGGATTCCAACAC, pCMV-NS1-R: GCGGATCCTCAAACCTTCTGACTCAAC, pCMV-p19-F: GCCGAATCCATGGAACGAGCTATACAAGGA, pCMV-p19-R: GCCGAGCTCTTACTCCCTTTCTTTTCGAA G and then inserted into the *EcoRI/BamHI* site and the *EcoRI/SacI* site in the pCMV-3 × Flag. All constructs generated by PCR were confirmed by nucleotide sequencing, and all of the plasmids described above were verified by restriction site analysis. Each construct was transformed into *Agrobacterium tumefaciens* GV3101 containing the helper plasmid pJIC SA Rep by the freeze–thaw method.

### Co-infiltration and GFP imaging

GFP-expressing *N. benthamiana* 16c plants with four to five leaves were infiltrated with the *A. tumefaciens* GV3101 strains carrying the above constructs according to the method of Jing et al. [26]. Local and systemic RNA silencing were examined through observing the GFP fluorescence in both the infiltrated leaves and newly emerging leaves under long-wave-length (365 nm) UV light (Spectroline model

SB-100P/A; UV Products, New York, NY), and photographs were taken with a CoolPix 5400 Nikon digital camera.

## RNA analysis

GFP mRNA and GFP siRNAs were extracted from leaf tissues and Northern blot analysis of GFP mRNA and GFP siRNAs used the method described by Jing et al. [26].

## siRNA and plasmid DNA transfections

We cultured Human renal epithelial 293T cells at 37 °C in Dulbecco's Modified Eagles Medium (HyClone, Los Angeles, USA) supplemented with 10% fetal bovine serum. Cells were harvested by trypsinization and plated on 60 mm tissue culture dishes at a density of  $4 \times 10^5$  to  $8 \times 10^5$  cells per  $\text{cm}^2$  with appropriate complete medium. Arrestin domain-containing protein-3 (*ARRDC3*) siRNAs (GGCCTGGCTAC TACCAGTdTdT and GCGTGGAATATTCACATAATdTdT) and three kinds of plasmid DNA (2 to 8  $\mu\text{g}$  total) were added to 200  $\mu\text{L}$  serum-free medium and mixed well. The mixture was incubated at 37 °C incubator for 4 h and then replaced with pre-warmed serum-containing medium. The cells were collected on 3, 5, and 7 days after transfection, respectively.

## RNA extraction and qPCR

Total RNA was extracted from the collected cells using TRIzol Reagent (Invitrogen, California, USA) following the manufacturer's instructions. cDNA was synthesized from 1  $\mu\text{g}$  of total RNA using TIANScript RT Kit (Tiangen, Beijing, China). Real-time quantitative polymerase chain reaction (RT-qPCR) was performed using Talent SYBR Green Kit (Tiangen, Beijing, China). Raw PCR data from Light-Cycler software 1.5.0 were analyzed. Specific primers for *ARRDC3* were GGCAGCCATTTACCAAAC and GAGGATAGAGGGAGAACTGG. Transcript levels were quantified in three independent biological replicates. Human *actin* was used as a housekeeping gene with primers CTCCATCCTGGCCTCGCTGT and GCTGTCACCTTCACCGTTCC.

## Results

### Sequence analysis of NS1 protein encoded by AIV H9N2

An RSS activity analysis of several NS1 subtypes showed that the variation in NS1 suppression activities among AIV strains seemed to contribute to differences in replication and pathogenicity of AIVs [27]. For instance, the NS1 protein encoded by AIV H1N1 was most efficient in suppressing RNA silencing mediated by short hairpin RNAs,

whereas the NS1 proteins in highly pathogenic H5N1 strains were more potent in compensating for the RSS function of Human immunodeficiency virus type I Tat protein [27]. Here, to clarify the RSS ability of the NS1 protein from low pathogenic AIV H9N2, the NS1 gene of the A/chicken/China/B1-6/2006 strain was amplified by reverse transcription PCR, and the cDNA of the NS1 gene was cloned and sequenced. We also compare the amino acid sequence of AIV H9N2 NS1(ACX48437) with NS1s from H3N2, H1N1, H7N7, and H5N1, which have been identified previously as RSSs. The result shows that the sequence homology of NS1 from each selected strain is very high at more than 77%. In particular, the RNA binding region (amino acids 19–41) is almost completely conserved. But the sequence homology is not directly related to the RNAi inhibition function of NS1. In addition, H9N2 and H5N1 NS1s can suppress type I interferon (IFN) induction, a characteristic function of NS1s in IAVs [28]. AIV H9N2 NS1 shares an almost identical sequence with A/HK/156/97 (H5N1) NS1 and 86.09% identity with the strongest RSS A/WSN/33 (H1N1) NS1 (Fig. 1).

### NS1 protein suppresses systemic RNA silencing induced by sense RNA or dsRNA

Our previous study showed that AIV H9N2 NS1 could suppress local RNA silencing caused by sense RNA and dsRNA [25]. To test whether the AIV H9N2 NS1 protein disturbs systemic RNA silencing triggered by sense green fluorescent protein (GFP), we monitored systemic GFP silencing in infiltrated plants under a hand-held UV light at 13 days post-infection (dpi). In most plants infiltrated with an empty vector, the newly emerging leaves lost GFP fluorescence in major veins, whereas that of the 19-kDa protein (p19) of *Tomato bushy stunt virus* (TBSV) and NS1-infiltrated plants retained green fluorescence (Fig. 2a). In agreement with this, a higher level of GFP mRNA was detected in emerging leaves from the areas of NS1 or p19 infiltrations than in plants infiltrated with an empty vector. As a major sign of RNA silencing, GFP siRNA could be detected at 13 dpi in the local and upper emerging leaves receiving empty vector and 35S-GFP. Nevertheless, GFP siRNA was nearly undetected in the local and upper emerging leaves infiltrated with 35S-GFP and 35S-NS1 or 35S-GFP and 35S-p19 at 13 dpi (Fig. 2b). The result also showed that the systemic RSS ability of NS1 was weaker than that of p19 (Fig. 2b). Furthermore, co-infiltrated patches and newly emerging leaves of the infiltrated plants were observed under a hand-held ultraviolet lamp from 3 to 35 dpi. A red ring on the edge of the infiltrated areas could be observed at 6 dpi in the areas of empty vector co-infiltrations, and at 13 dpi in the areas of NS1 and p19 co-infiltrations (date not shown). Almost all empty vector-infiltrated plants revealed typical GFP silencing in the areas adjacent to the veins of emerging

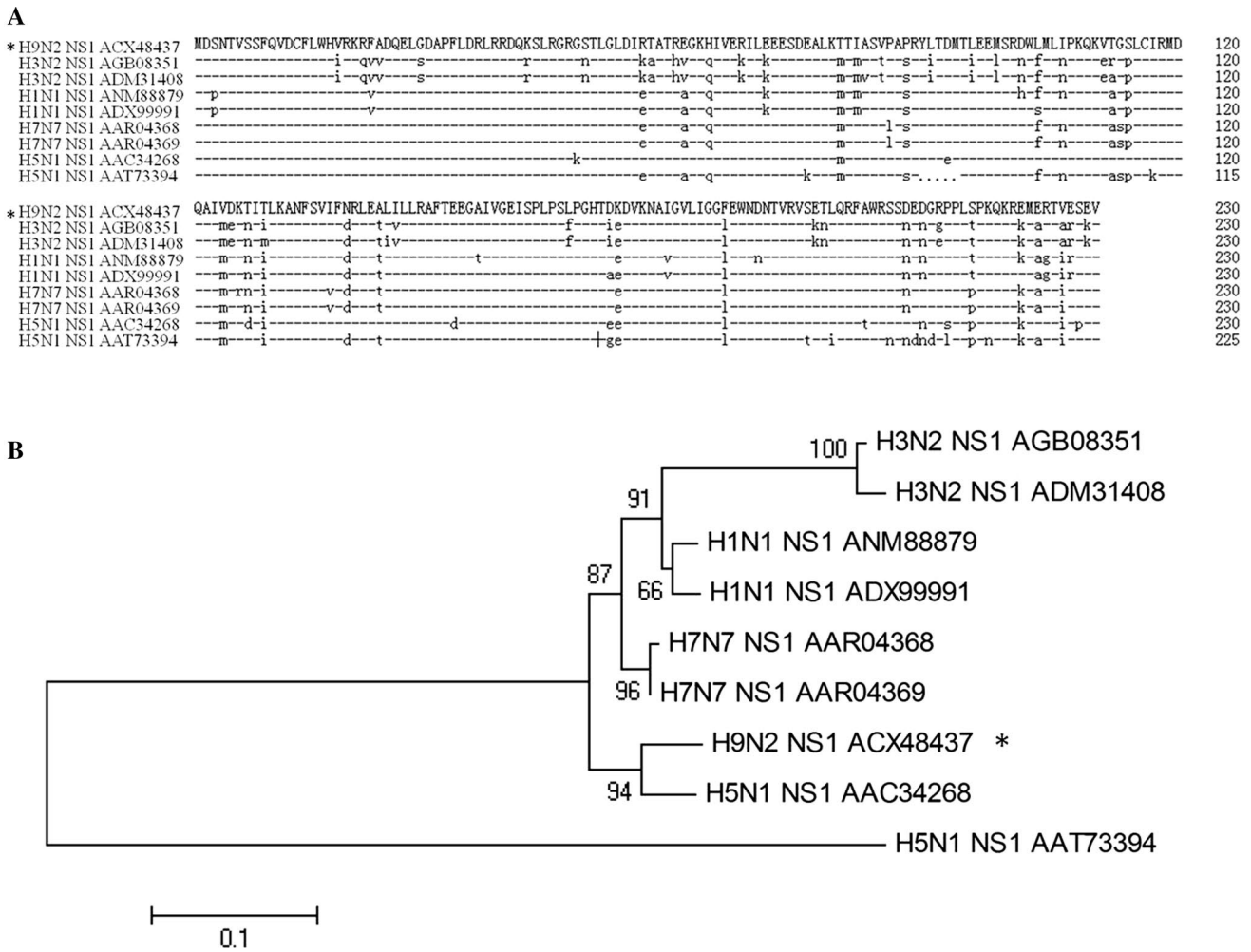


**Fig. 1** NS1 sequences of different AIV strains. **a** Sequence alignment of NS1 proteins. Complete amino acid sequences of NS1s from different AIV strains were compared by DNAMAN. Dashes indicate residues identical to those of AIV H9N2 NS1 and dots indicate deletions. **b** A phylogenetic tree of NS1 proteins. A highly resolved, automati-

cally phylogenetic tree of NS1 proteins generated using MEGA4.0, based on complete amino acid sequences of NS1s from different strains of influenza virus. The asterisk marks the target protein of this study

leaves at 10 dpi. However, systemic GFP silencing in NS1 co-infiltrations was observed until 15 dpi. It was stronger in the upper leaves at 21 dpi, and extended to the whole plant at 28 dpi (Fig. 2c).

To further test whether the AIV H9N2 NS1 protein suppresses systemic RNA silencing induced by dsGFP, we measured the effects of NS1 on systemic RNA silencing triggered by GFP dsRNA. At 13 dpi, strong systemic GFP silencing occurred in the plants with empty vector infiltrations, whereas strong green fluorescence was maintained in those with NS1 or p19 infiltration (Fig. 2d). In addition, the intensity of green fluorescence in the newly emerging leaves of plants with NS1 infiltrations was significantly weaker than that of plants with p19 infiltrations (Fig. 2d). We also followed GFP expression in local tissues until 13 dpi, and there was still strong green fluorescence in plants with NS1 and

p19 infiltrations (Fig. 2e). Results showing GFP mRNA and siRNA accumulation were supported by visual observations (Fig. 2e). These results suggest that AIV H9N2 NS1 can suppress systemic silencing triggered by sense GFP RNA or GFP dsRNA. Suppressing RNA silencing triggered by sense RNA or dsRNA indicates that NS1 likely targets a downstream step in dsRNA formation at an early stage in the RNA silencing process.

**NS1 protein could cause more severe PVX symptoms, although it could not reverse the established systemic GFP silencing**

The PVX vector has low suppression activity and the inability to reverse RNA silencing in co-infiltrations. Therefore, we used the heterologous vector PVX to validate the



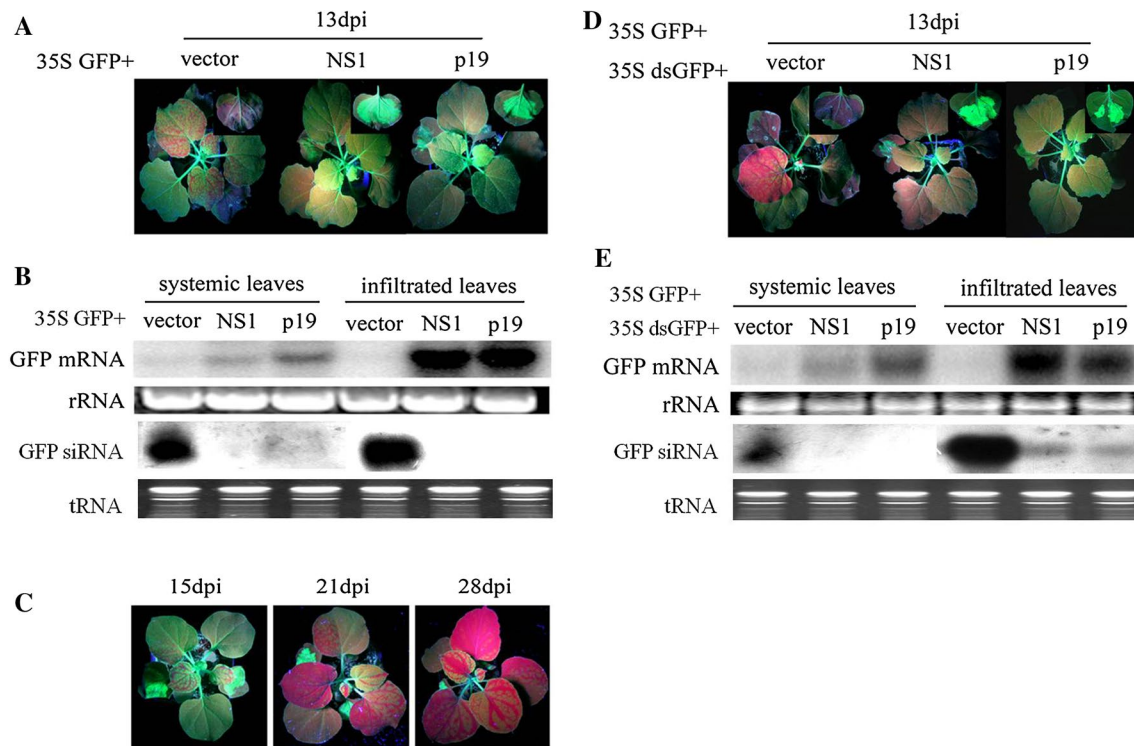


**Fig. 2** Effect of avian influenza virus H9N2 NS1 protein on systemic GFP silencing triggered by sense RNA and dsRNA. **a** Co-infiltration of transgenic *N. benthamiana* 16c leaves with 35S-GFP and empty vector, 35S-NS1 or 35S-p19. **d** Co-infiltration in 16c leaves with 35S-GFP, 35S-dsGFP, and empty vector, 35S-NS1 or 35S-p19. Images were obtained under a hand-held long-wave ultraviolet lamp at 13 dpi. The inserted photographs show the local silencing of infiltrated patches (top right). **b**, **e** Northern blot assays of green fluores-

cent protein (GFP) mRNA and siRNA extracted from local and distal leaves of plants co-infiltrated with the strains mentioned above at 13 dpi. Ethidium bromide-stained rRNA was used as a loading control for mRNA. **c** Photographs of 16c plants infiltrated with *Agrobacterium tumefaciens* harboring 35S-GFP and 35S-NS1 at 15, 21, and 28 dpi obtained under a hand-held long-wave ultraviolet lamp (Color figure online)

silencing suppression activity of H9N2 NS1. To determine whether NS1 can reverse GFP silencing, a silencing-inducing single-sense GFP containing plasmid was first allowed to infiltrate 16c, and then a PVX vector (pGR106) harboring NS1 was inoculated into the upper leaves at 18 dpi, when silencing occurred in the entire plant. No GFP fluorescence was observed in patches inoculated with the PVX-vector or PVX-NS1 at 7 dpi, whereas green fluorescence was found in patches inoculated with PVX-p19 (Fig. 3a). Consistent with these observations, northern blot assays of GFP mRNA extracted from infected local leaves at 7 dpi showed that there was little GFP mRNA in the leaves exposed to the PVX-vector or PVX-NS1 infiltrations, whereas abundant GFP mRNA was detected in PVX-p19-infiltrated leaves (Fig. 3b). These results suggested that NS1 could not reverse established systemic GFP silencing. This is consistent with the finding of Delgado et al. [18], but differs from results of a study by Bucher et al. [29]. We suspect that although NS1s are highly homologous, small differences in sequence can

result in different RSS activities. This is supported by the studies on the differential RSS activities of NS1 proteins encoded by various IAV strains [27].

AIV H9N2 NS1 protein could not reverse established systemic GFP silencing in emerging leaves, but it did cause more severe PVX symptoms. We found that PVX-NS1 caused more severe symptoms than PVX-vector at 7 and 20 dpi (Fig. 3c, d), a phenomenon often observed in suppressor-expressing plants [30]. Co-infiltration of 35S-GFP and PVX-NS1 caused cell death as early as 7 dpi (Fig. 3c), and the leaves were entirely dried by 20 dpi (Fig. 3d). We speculated that NS1 acted as an RSS to promote the accumulation of PVX by being stably expressed in viral progeny. As early as 2004, Bucher and Delgado showed that a PVX vector expressing human influenza virus NS1 protein caused more severe symptoms than a PVX vector with no insertion in various plant hosts [18, 29]. Similarly, a study of Munir et al. showed that expressing the NS1 gene in a low pathogenic H9N2 virus strain increased the pathogenicity of the virus [28].

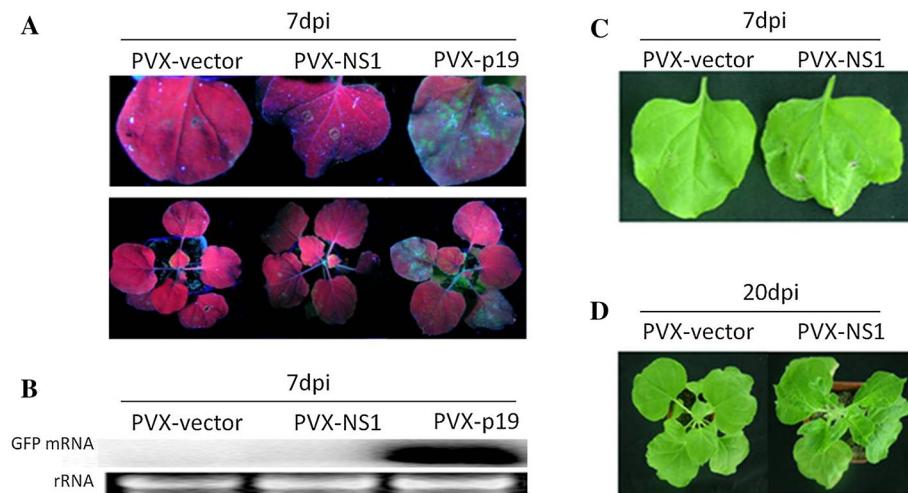


**Fig. 3** Verification of avian influenza virus H9N2 NS1 suppressor activity using silenced *N. benthamiana* 16c and the heterologous PVX vector. **a** Reversion of green fluorescent protein (GFP) silencing by NS1. 16c plants were firstly infected with an *Agrobacterium* strain carrying 35S-GFP, and lost green fluorescence at 18 days post-infection (dpi). Then, PVX-vector, PVX-NS1, and PVX-p19 were inoculated into the upper leaves of these plants, and photographs of these

leaves were obtained at 7 days after the second infiltration under UV illumination. **b** Northern blot assays of GFP mRNA extracted from infected local leaves (**a**) at 7 dpi. Ethidium bromide-stained rRNA was used as a loading control for mRNA. Phenotypic effects of infection with PVX-NS1 or PVX-vector in *N. benthamiana* plants at 7 dpi (**c**) and 20 dpi (**d**) (Color figure online)

### Comparison of the RNA silencing suppression activity of NS1 with p19

Studies on the functional structure of RSSs can help identify the interactions between virus and host. TBSV p19 has a well-defined structure and is widely used as a suppressor [31, 32]. Experiments in vitro have shown that p19 can bind 21nt siRNAs, despite not containing a conserved dsRNA binding motif [33]. p19 is believed to prevent the formation of RISC by sequestering viral siRNAs [32]. Previous research has shown that AIV H9N2 NS1 can effectively suppress local RNA silencing, similar to p19 [25]. Therefore, we compared the local silencing suppression capacity of NS1 with that of p19. Local GFP silencing in infiltrated plants was monitored using a hand-held UV light at 3, 5, 7, 10, and 17 dpi (Fig. 4a). In almost all empty vector-infiltrated plants, weak GFP fluorescence was observed in infiltrated patches at 3 dpi. This fluorescence disappeared at 5 dpi, turned red at 7 dpi, and remained significantly red from 10 to 17 dpi (Fig. 4a). As a result of silencing suppression, the leaves co-infiltrated with 35S-GFP and 35S-NS1 or 35S-p19 continued to exhibit bright GFP fluorescence from 3 to 17 dpi (Fig. 4a). Northern blot assays of GFP mRNA showed that little GFP mRNA accumulated in the leaves expressing GFP and the empty vector at 3 dpi, and GFP mRNA was nearly undetectable from 5 to 17 dpi. By contrast, the levels of steady-state GFP mRNA were dramatically higher in the leaves expressing GFP and NS1 or p19 from 3 to 17 dpi. GFP mRNA accumulation of NS1 co-infiltrations was less than that of p19 at 3 dpi, almost the same as p19 at 5 dpi, markedly higher than that of p19 from 7 to 10 dpi, and

then little less than that of p19 at 17 dpi (Fig. 4b). These results showed that the local RSS activity of NS1 was significantly stronger than that of p19 from 7 to 10 dpi, and, at other times, was weaker than or equivalent to that of p19.

To compare the RSS activity between NS1 and P19 in animal cells, *ARRDC3* siRNA were transfected into human renal epithelial 293T cells with pCMV-NS1 or pCMV-p19, respectively. Cells co-transfected with *ARRDC3* siRNA and empty pCMV were taken as control. The cells were collected at 3, 5, and 7 days after transfection, respectively. The RT-PCR results showed that the expression of *ARRDC3* in the cells transfected with NS1 was significantly higher than the control, indicating that NS1 also plays a role of suppressing RNAi in human cells (Fig. 5). And NS1 presented the strongest suppression on RNAi at 3 days after transfection during the test phase. Some studies have shown that p19 can effectively inhibit RNAi in animal cells such as *Drosophila*, and mammalian cells [10, 34]. The experimental results also showed that the expression of *ARRDC3* mRNA in the cells transfected p19 was significantly higher than that of the control (Fig. 5). The expression of *ARRDC3* in the cells transfected NS1 was always higher than that of p19 during the test phase (Fig. 5).

### Discussion

Studies have shown that the p19 protein is composed of four  $\beta$ -sheets and five  $\alpha$ -helices and forms a homodimer when it is bound to siRNA in a cell. Two  $\alpha$ -helices

**Fig. 4** RNA silencing suppression activity comparison between NS1 and p19. **a** Co-infiltrations of 16c leaves with *Agrobacterium* and 35S-GFP and the empty vector or constructs expressing NS1 or p19. Photographs were obtained under UV light at 3, 5, 7, 10, and 17 days post-infection (dpi). **b** Northern blot assays of GFP mRNA extracted from leaves co-infiltrated with the various strains at 3, 5, 7, 10, and 17 dpi. Ethidium bromide-stained rRNA was used as a loading control for mRNA. This assay was repeated two times with five plants per replicate

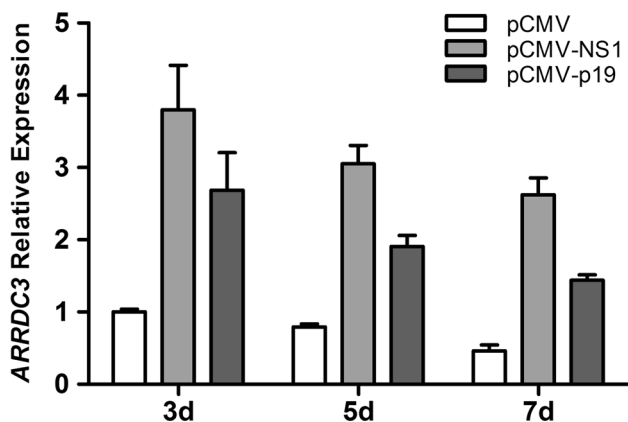
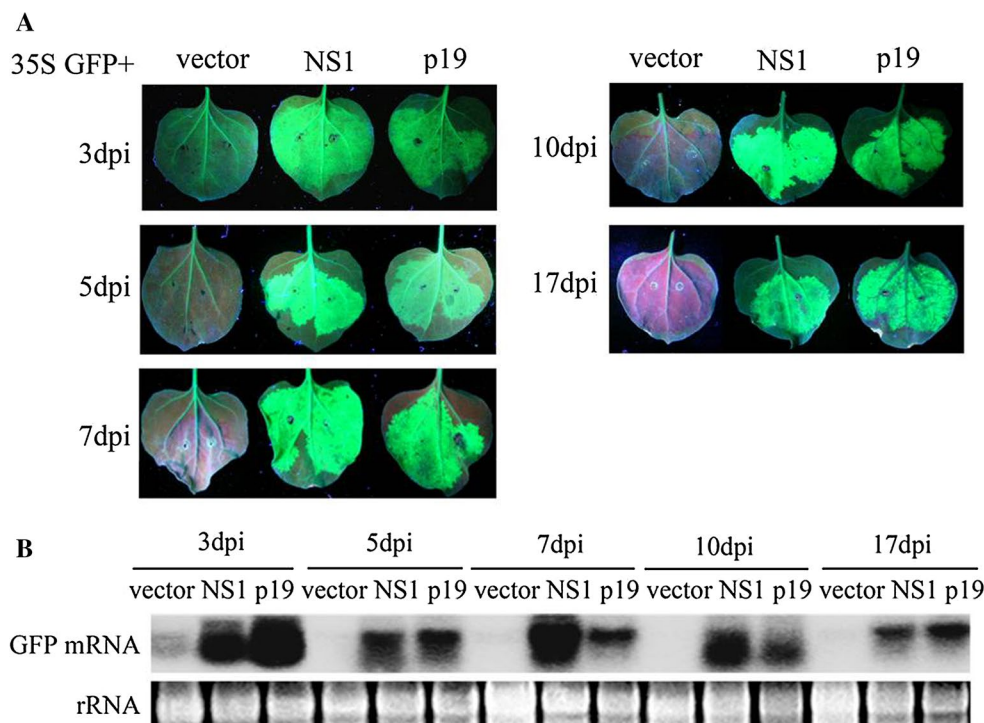


**Fig. 5** RNA silencing suppression activity of NS1 and p19 in human cells. *ARRDC3* siRNA was co-transfected into human T293 cells with pCMV, pCMV-NS1 or pCMV-p19. The cells were collected at 3, 5, and 7 days after transfection, respectively, for total RNAs extraction. *ARRDC3* mRNA levels were determined by RT-qPCR. Transcript levels were normalized relative to that of the *actin* gene. Data points show the mean  $\pm$  SD of three replicate assays

protrude from the homodimer ends and position tryptophan pairs over the terminal base pairs, thereby determining the size of the siRNA duplex. This is why p19 binds preferentially to 21 nt siRNAs rather than to longer siRNAs [35]. Similarly, as an RNA binding protein, NS1 not only binds siRNA but also recognizes longer dsRNAs [18, 36]. In animals, larger dsRNA molecules, as well as siRNAs, have been shown to be involved in the

sequence-unspecific initiation of an IFN-mediated innate antiviral response [37, 38]. This might explain the above observations for different RSS activities of NS1 at various post-infiltration times. Therefore, when NS1 protein was used as a tool to enhance exogenous gene expression, choosing the right time for observation is of great importance.

Viral RSS proteins are important factors of pathogenicity in plants. Similarly, NS1 is the major virulence determinant in influenza viruses. Most AIV subtypes do not result in severe disease in poultry, whereas some subtypes are associated with pandemics [39, 40]. Previous studies have shown that RSS activity is cell-line dependent [41]. NS1 was reported to have the function of suppressing RNA silencing in animals [21]. This experiment demonstrated that H9N2 NS1 functions as a more potent RSS in human cells even more effective than p19. This indicated the RNA silencing suppression mechanisms of NS1 in plants and animals might be very different. Apart from the RSS activity of NS1 protein, the other functions of NS1 in the interactions between virus and host should not be overlooked. Previous studies have shown that gene mutations in NS1, namely F103L and M106I, enhanced protein synthesis and virus virulence [28, 42]. NS1 protein can inhibit type I IFN responses as well as RNA silencing—two main defence mechanisms in mammalian cells that are mediated by dsRNA. A detailed understanding of RSS function and RNA binding characteristics of NS1 may aid in manipulating RNA silencing and the IFN response to limit influenza virus infections.

**Acknowledgements** We thank Prof. David Baulcombe for providing *N. benthamiana* 16c seeds and the p19 gene and Prof. Zhizhong Cui for providing the avian influenza virus H9N2 strain. And thanks are due to Dr. Zizhang Zhou and Dr. Haifang Li for the assistance in animal experiments. This work was supported by grants from the Natural Science Foundation of Shandong Province [ZR2015CM018] and National Natural Science Foundation of China [31272113 and 31300730].

**Author contributions** RY and XJ performed the main experiments and edited the paper; CZ participated in experimental design; JX, WL, YX, and LG were involved in executing the study; HL guided the execution of the study and revised the paper.

## Compliance with ethical standards

**Conflict of interest** The authors declare no conflict of interest.

**Human and animal consent** The research described in the paper does not use any human or animal subjects.

## References

1. S.W. Ding, Nat. Rev. Immunol. **10**, 632–644 (2010)
2. D. Baulcombe, Trends Microbiol. **10**, 306–308 (2002)
3. W.X. Li, S.W. Ding, Curr. Opin. Biotechnol. **12**, 150–154 (2001)
4. L. Lakatos, T. Csorba, V. Pantaleo, E.J. Chapman, J.C. Carrington, Y.P. Liu, V.V. Dolja, L.F. Calvino, J.J. Lopez-Moya, J. Burgyan, EMBO J. **25**, 2768–2780 (2006)
5. Z. Merai, Z. Kerenyi, S. Kertesz, M. Magna, L. Lakatos, D. Silhavy, J. Virol. **80**, 5747–5756 (2006)
6. K. Goto, T. Kobori, Y. Kosaka, T. Natsuaki, C. Masuta, Plant Cell Physiol. **48**, 1050–1060 (2007)
7. S. Hamera, X. Song, L. Su, X. Chen, R. Fang, Plant J. **69**, 104–115 (2012)
8. X. Zhang, Y.R. Yuan, Y. Pei, S.S. Lin, T. Tuschl, D.J. Patel, N.H. Chua, Genes Dev. **20**, 3255–3268 (2006)
9. H. Li, W.X. Li, S.W. Ding, Science **296**, 1319–1321 (2002)
10. W.X. Li, H. Li, R. Lu, F. Li, M. Dus, P. Atkinson, E.W. Brydon, K.L. Johnson, A. Garcia-Sastre, L.A. Ball, P. Palese, S.W. Ding, Proc Natl. Acad. Sci. USA **101**, 1350–1355 (2004)
11. J.A. Richt, A. Garcia-Sastre, Curr. Top. Microbiol. Immunol. **333**, 177–195 (2009)
12. S.H. Seo, E. Hoffmann, R.G. Webster, Virus Res. **103**, 107–113 (2004)
13. J.J. Skehel, Virology **49**, 23–36 (1972)
14. T. Horimoto, Y. Kawaoka, Nat. Rev. Microbiol. **3**, 591–600 (2005)
15. J.C. Obenauer, J. Denson, P.K. Mehta, X. Su, S. Mukatira, D.B. Finkelstein, X. Xu, J. Wang, J. Ma, Y. Fan, K.M. Rakestraw, R.G. Webster, E. Hoffmann, S. Krauss, J. Zheng, Z. Zhang, C.W. Naeye, Science **311**, 1576–1580 (2006)
16. V. Balme-Sinibaldi, M. Tribodet, F. Croizat, P. Lefeuvre, C. Kerlan, E. Jacquot, J. Virol. Methods **134**, 261–266 (2006)
17. D. Lin, J. Lan, Z. Zhang, Acta Biochim. Biophys. Sin. **39**, 155–162 (2007)
18. M.O. Delgadillo, P. Saenz, B. Salvador, J.A. Garcia, C. Simon-Mateo, J. Gen. Virol. **85**, 993–999 (2004)
19. V.I. Maliogka, M. Calvo, A. Carbonell, J.A. Garcia, A. Valli, J. Gen. Virol. **93**, 1601–1611 (2012)
20. J. Brask, A. Chauhan, R.H. Hill, H.G. Ljunggren, K. Kristensson, J. Neurovirol. **11**, 395–402 (2005)
21. K. Melen, L. Kinnunen, R. Fagerlund, N. Ikonen, K.Y. Twu, R.M. Krug, I. Julkunen, J. Virol. **81**, 5995–6006 (2007)
22. E.M. Kennedy, A.W. Whisnant, A.V. Kornepati, J.B. Marshall, H.P. Bogerd, B.R. Cullen, Proc. Natl. Acad. Sci. USA **112**, E6945–E6954 (2015)
23. Y. Li, M. Basavappa, J. Lu, S. Dong, D.A. Cronkite, J.T. Prior, H.C. Reinecker, P. Hertzog, Y. Han, W.X. Li, S. Cheloufi, F.V. Karginov, S.W. Ding, K.L. Jeffrey, Nat. Microbiol. **2**, 16250 (2016)
24. A. Cheng, S.M. Wong, Y.A. Yuan, Cell Res. **19**, 187–195 (2009)
25. X. Jing, J. Xu, M. Fan, L. Ma, X. Huang, X. Wang, S. Sun, C. Zhu, H. Liu, J. Gen. Virol. **96**, 1613–1618 (2015)
26. X.L. Jing, M.N. Fan, G. Jia, L.W. Liu, L. Ma, C.C. Zheng, X.P. Zhu, H.M. Liu, X.Y. Wang, J. Virol. **85**, 12792–12803 (2011)
27. W. de Vries, J. Haasnoot, R. Fouchier, P. de Haan, B. Berkhout, J. Gen. Virol. **90**, 1916–1922 (2009)
28. M. Munir, S. Zohari, M. Iqbal, M. Abbas, D.R. Perez, M. Berg, Virulence **4**, 612–623 (2013)
29. E. Bucher, H. Hemmes, P. de Haan, R. Goldbach, M. Prins, J. Gen. Virol. **85**, 983–991 (2004)
30. G. Brigneti, O. Voinnet, W.X. Li, L.H. Ji, S.W. Ding, D.C. Baulcombe, EMBO J. **17**, 6739–6746 (1998)
31. H.B. Scholthof, Nat. Rev. Microbiol. **4**, 405–411 (2006)
32. D. Silhavy, J. Burgyan, Trends Plant Sci. **9**, 76–83 (2004)
33. D. Silhavy, A. Molnar, A. Luciola, G. Szittyta, C. Hornyik, M. Tavazza, J. Burgyan, EMBO J. **21**, 3070–3080 (2002)
34. R.P. van Rij, M.C. Salch, B. Berry, C. Foo, A. Houk, C. Antoniewski, R. Andino, Genes Dev. **20**, 2985–2995 (2006)
35. K. Ye, L. Malinina, D.J. Patel, Nature **426**, 874–878 (2003)
36. X. Chen, Annu. Rev. Cell Dev. Biol. **25**, 21–44 (2009)
37. C.A. Sledz, M. Holko, M.J. de Veer, R.H. Silverman, B.R. Williams, Nat. Cell Biol. **5**, 834–839 (2003)
38. A.J. Bridge, S. Pebernard, A. Ducraux, A.L. Nicoulaz, R. Iggo, Nat. Genet. **34**, 263–264 (2003)
39. D. Jackson, M.J. Hossain, D. Hickman, D.R. Perez, R.A. Lamb, Proc. Natl. Acad. Sci. USA **105**, 4381–4386 (2008)
40. S.H. Seo, E. Hoffmann, R.G. Webster, Nat. Med. **8**, 950–954 (2002)
41. J. Haasnoot, W. de Vries, E.J. Geutjes, M. Prins, P. de Haan, B. Berkhout, PLoS Pathog. **3**, E86 (2007)
42. S.K. Dankar, S. Wang, J. Ping, N.E. Forbes, L. Keleta, Y. Li, E.G. Brown, J. Virol. **8**, 13 (2011)